

Radio-mm-FIR Photometric Redshifts for (sub-)mm Galaxies

Itziar Aretxaga¹, David H. Hughes¹, James S. Dunlop²

¹*Instituto Nacional de Astrofísica, Óptica y Electrónica
Aptdo. Postal 51 y 216, 72000 Puebla, Mexico.*

²*Institute for Astronomy, University of Edinburgh, Royal Observatory,
Edinburgh, EH9 3HJ, UK.*

Abstract. We present a comparison between the published optical, IR and CO spectroscopic redshifts of 86 (sub-)mm galaxies and their photometric redshifts as derived from long-wavelength (radio-mm-FIR) photometric data. The redshift accuracy measured for 13 sub-mm galaxies with at least one robustly-determined colour in the radio-mm-FIR regime and additional constraining upper limits is $\Delta z \approx 0.30$. This accuracy degrades to $\Delta z \approx 0.65$ when only the 1.4GHz/850 μ m spectral index is used, as derived from the analysis of a subsample of 58 galaxies with robustly determined redshifts. Despite the wide range of spectral energy distributions in the local galaxies that are used in an un-biased manner as templates, this analysis demonstrates that photometric redshifts can be efficiently derived for sub-mm galaxies with a precision of $\Delta z < 0.5$ using only the rest-frame FIR to radio wavelength data, sufficient to guide the tuning of broad-band heterodyne observations (e.g. 100mGBT, 50mLMT, ALMA) or aid their determination in the case of a single line detection by these experiments.

1. Introduction

The next generation of wide-area extragalactic submillimetre and millimetre surveys, will produce large samples ($\sim 10^3 - 10^5$) of distant, luminous starburst galaxies. The dramatic increase in the number of detected galaxies makes it necessary to identify a selection technique that can efficiently generate redshift selected subsamples that are then explored in greater detail with optical/IR and mm follow-up facilities, such as ALMA.

Given the underlying assumption that we are witnessing high rates of star formation in these (sub-)millimetre galaxies (see Blain, in this volume), then we expect them to have the characteristic FIR peak and steep submillimetre (Rayleigh-Jeans) spectrum which is dominated by thermal emission from dust grains heated to temperatures in the range $\sim 20 - 70$ K by heavily obscured young, massive stars. The observed radio-FIR luminosity correlation in local starburst galaxies (e.g. Helou, Soifer & Rowan-Robinson 1985), that links the radio synchrotron emission from supernova remnants with the later stages of massive star formation, is also expected to apply to these galaxies.

Thus, in recent years, a considerable amount of effort has been invested in assessing the accuracy with which these broad continuum features in the spectral energy distributions (SEDs) of submillimetre galaxies, at rest-frame mid-IR to radio wavelengths can be used to provide photometric-redshifts (Hughes et al.

1998; Carilli & Yun 1999, 2000; Dunne, Clements & Eales 2000; Rengarajan & Takeuchi 2001; Yun & Carilli 2002; Hughes et al. 2002, Aretxaga et al. 2003, 2005; Wiklind 2003; Blain, Barnard & Chapman 2003; Hunt & Maiolino 2005; Laurent et al. 2006).

This paper is an update on previous work (Aretxaga et al. 2005) that assessed the accuracy of the FIR-mm-radio photometric redshift techniques given the larger samples of spectroscopic redshifts recently published in the literature (see Chapman and Tacconi, in this volume, and references therein, for the primary sources of comparison data).

The cosmological parameters adopted throughout this paper are $H_0 = 67 \text{ km s}^{-1} \text{ Mpc}^{-1}$, $\Omega_M = 0.3$, $\Omega_\Lambda = 0.7$.

2. Accuracy of the 1.4GHz/850 μm spectral index as a redshift diagnostic

The 1.4GHz/850 μm spectral index is discussed following 3 different prescriptions: the one-template maximum-likelihood technique originally designed by Carilli & Yun (1999, 2000), denoted as $z_{\text{phot}}^{\text{CY}}$; a maximum likelihood technique which simultaneously fits the 20 local templates of starbursts, ULIRGs and AGN used by Aretxaga et al. (2003, 2005), denoted as $z_{\text{phot}}^{\text{A}}$; and a multi-template maximum-likelihood technique that uses the 3 blue compact dwarf SEDs of Hunt & Maiolino (2005) that reproduce the radio-mm-FIR data of sub-mm galaxies (the templates for NGC 5253, and two flavours of II Zw 40 SEDs with radio slopes $\alpha = -0.5$ and -0.1), which we denote as $z_{\text{phot}}^{\text{HM}}$. For all three techniques the error bars of the photometric redshifts were derived by bootstrapping on the reported photometric and calibration errors and, in the case of $z_{\text{phot}}^{\text{CY}}$, the error estimated by Carilli & Yun (2000), to allow for a difference in templates, is added in quadrature to the errors derived by bootstrapping the photometry.

We have assembled a sample of 86 objects which have published optical/IR or CO spectroscopic redshifts (z_{spec}) and accompanying photometry to assess the accuracy of the techniques described in this paper.

Using the 1.4GHz to 850 μm color ratio and the $z_{\text{phot}}^{\text{A}}$ prescription, we find a mean accuracy of $z_{\text{phot}}^{\text{A}} - z_{\text{spec}} \sim 0.65$ (Fig. 1) for a robust sub-sample of objects with undisputed interpretation about their optical/IR/radio counterparts and spectroscopic redshifts derived from the identification of more than two spectral features. This subsample does not include powerful radio-loud AGN, for which the templates used in the photometric redshift analysis are not appropriate. Restricting the analysis only to those galaxies with CO spectroscopic redshifts, the measured accuracy is $z_{\text{phot}}^{\text{A}} - z_{\text{spec}} \sim 0.6$. The error distribution for the sample of galaxies is centered at -0.15 , which we do not regard as significant as it is well below the resolution used in the Monte Carlo simulations that aid the calculation of the photometric redshifts. The precision degrades as the redshift increases, as expected from the 1.4GHz/850 μm spectral index, which flattens beyond $z = 3$ (Carilli & Yun 2000), leading to a measured $z_{\text{phot}}^{\text{A}} - z_{\text{spec}} \sim 1.0$ at $3 \leq z \leq 4$. Using all objects with published photometry, regardless of whether the spectroscopic redshift is suspected to be incorrect or not, or is not regarded

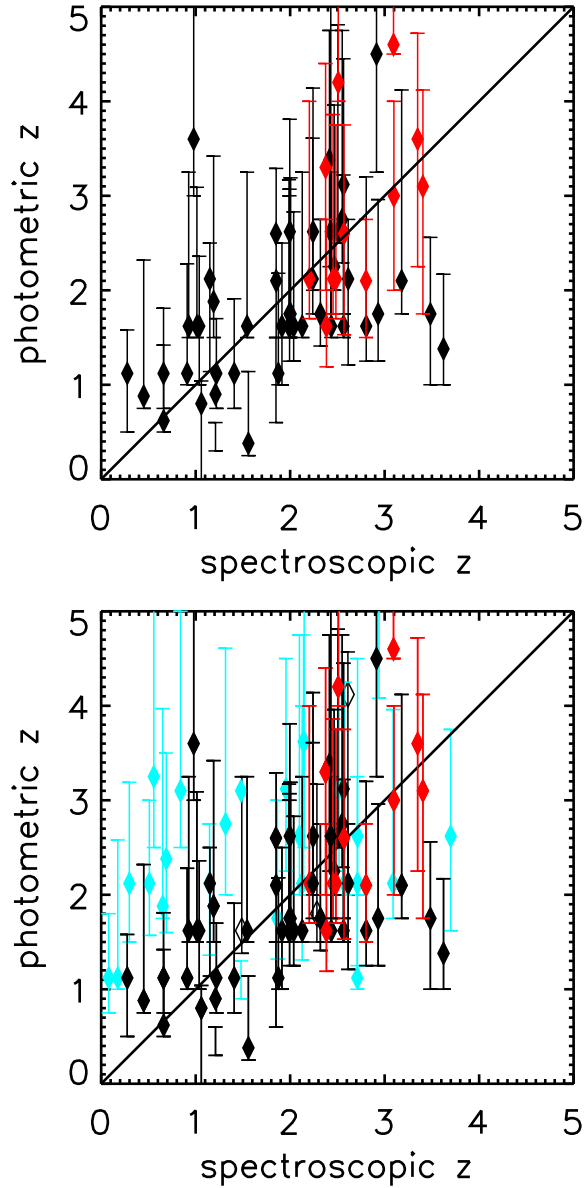


Figure 1. Comparison of spectroscopic and photometric redshifts derived from the 1.4GHz/850 μ m spectral index for a sample of 86 galaxies. **(Top)** Robust sample of undisputed radio/optical/IR counterpart associations of the sub-mm galaxies, and spectroscopic redshifts derived from 2 or more lines: in dark grey, CO confirmed optical/IR spectroscopic redshifts; and in black, redshifts based on optical/IR spectra with two or more characteristic emission or atmospheric/winds absorption lines. The error bars represent 68% confidence intervals in the determination of the redshift, and the diamonds the mode of the distributions. **(Bottom)** The same for all 86 galaxies, where empty symbols represent optical/IR redshifts that have failed to obtain confirmation with CO observations, and light grey symbols are redshifts that have been disputed in the literature or that are based on only one characteristic line, and thus are not considered robust enough to be included in the sample above.

as robustly determined, the overall accuracy over the $0 \leq z \leq 4$ regime degrades to $\Delta z = 0.8$.

We find that for the same robust sample of objects, $z_{\text{phot}}^{\text{CY}}$ has systematically larger errors, $\Delta z \sim 0.9$, while the $z_{\text{phot}}^{\text{HM}}$ provides a similar $\Delta z \sim 0.7$ dispersion compared to the results of $z_{\text{phot}}^{\text{A}}$. The $z_{\text{phot}}^{\text{HM}}$ prescription gives, however, poorer estimations of the redshift for the CO confirmed sources ($\Delta z \sim 0.85$) than the $z_{\text{phot}}^{\text{A}}$ technique ($\Delta z \sim 0.6$).

3. Fitting the full rest-frame radio-FIR SED

For a few tens of sources, multiwavelength data in the radio to FIR regime is available, beyond the 1.4GHz and 850 μm photometry. These additional data can also be used to place extra constraints on the redshift of the sources by sampling the FIR bump. This information has been exploited by several groups, including our own, using a wide array of fitting techniques and SEDs (e.g. Yun & Carilli 2002, Wiklind 2003, Laurent et al. 2006). Our own particular technique is based on Monte-Carlo simulations to also take into account constraining prior information such as the number counts of submm galaxies, the favoured luminosity/density evolution up to $z \approx 2$, and the amplification or clustering of a certain field (Hughes et al. 2002, Aretxaga et al. 2003, 2005). We only offer a brief summary of the technique here. We generate a catalogue of 60 μm luminosities and redshifts for mock galaxies from an evolutionary model for the 60 μm luminosity function that fits the observed 850 μm number-counts. Randomly-selected template SEDs are drawn from a library of local starbursts, ULIRGs and AGN, to provide FIR–radio fluxes. The SEDs cover a wide-range of FIR luminosities ($9.0 < \log L_{\text{FIR}}/L_{\odot} < 12.3$) and temperatures ($25 < T/K < 65$). The fluxes of the mock galaxies include both photometric and calibration errors, consistent with the quality of the observational data for the sub-mm galaxy detected in a particular survey. We reject from the catalogue those mock galaxies that do not respect the detection thresholds and upper-limits of the particular sub-mm galaxy under analysis. The redshift probability distribution of a sub-mm galaxy is then calculated as the normalized distribution of the redshifts of the mock galaxies in the reduced catalogue, weighted by the likelihood of identifying the colours and fluxes of each mock galaxy with those of the sub-mm galaxy in question.

Fig. 2 shows an example of our method for LH850.1, the brightest source of the SCUBA 8mJy survey in Lockman Hole field (Scott et al. 2002, Ivison et al. 2002, Greve et al. 2004, Laurent et al. 2005, 2006), that tentatively has been assigned the optical/IR spectroscopic redshift of a plausible counterpart at $z_{\text{spec}} = 2.15$ (Chapman et al. 2005, Ivison et al. 2005).

Using the full SED information of a robust sub-sample of 13 objects (Fig. 3) with undisputed identification of their optical/IR/radio counterparts and spectroscopic redshifts derived from the measurement of two spectral features or more, we find a mean accuracy of $z_{\text{phot}}^{\text{A}} - z_{\text{spec}} \sim 0.3$. Restricting the analysis only to those 5 galaxies with CO spectroscopic redshifts, the measured accuracy is $z_{\text{phot}}^{\text{A}} - z_{\text{spec}} \sim 0.1$. The error distribution for the robust sample of galaxies is centered in $\Delta z = +0.17$, which is within the resolution afforded by the Monte

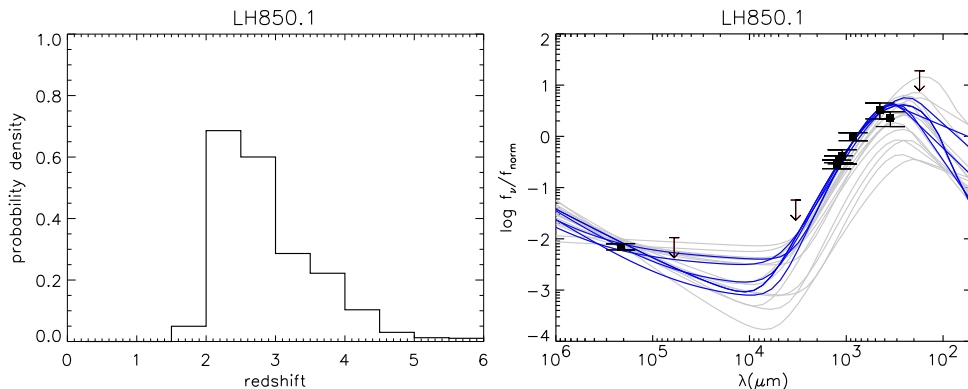


Figure 2. **Left** Redshift probability density distribution derived for LH850.1. The probability density peaks at $z \approx 2.4$ (as seen in higher resolution simulations). **Right** The observed SED of LH850.1 normalised to the flux density at $850\mu\text{m}$ is shown as squares (detections) and arrows (3σ upper limits). The template SEDs (lines) are redshifted to the spectroscopic redshift $z = 2.15$ and scaled in flux to fit the points and arrows through survival analysis. The template SEDs *at this redshift*, compatible within the 3σ error bars with the SED of LH850.1, are displayed as darker lines. A fit at $z = 2.4$ also selects 5 compatible SEDs with the photometry of the object, yielding a figure that is almost indistinguishable from this one by eye.

Carlo simulations that aid the photometric redshifts. In contrast with the simple $1.4\text{GHz}/850\mu\text{m}$ spectral index, the precision does not degrade as the redshift increases. Three extra galaxies can be included in the same analysis, that have not been confirmed by a CO detection at the published optical/IR spectroscopic redshift. This could be due to an erroneous redshift or insufficient sensitivity in the search for a CO line. Including these 3 objects in the analysis, we find an overall precision of $\Delta z = 0.3$. Using all objects with published photometry, regardless of whether the spectroscopic redshift is questioned or not, the overall accuracy over the $0 \leq z \leq 4$ regime degrades to $\Delta z = 0.65$, with some significant outliers (lower panel of Fig. 3).

The two outliers at the lowest redshift correspond to LH850.8 (at $z_{\text{spec}} = 0.689$) and N2850.1 (at $z_{\text{spec}} = 0.840$), and their observed SEDs cannot be reproduced by any of the SED templates in our library at the published spectroscopic redshift (Fig. 4, see also Aretxaga et al. 2005 and Laurent et al. 2006), or by the blue compact dwarf SEDs of Hunt & Maiolino, which have been claimed to provide better fits to the overall sub-mm galaxy photometry than those of giant star-forming galaxies — although the inspection of Fig.4, shows that these three templates lie within the range of the templates of ULIRGs, AGN and local star-forming galaxies used in Aretxaga et al (2003). The robustness of the optical associations for N2850.1 and LH850.8 has been questioned in the literature (Chapman et al. 2002, Ivison et al. 2005). Apart from a true association, it also has been suggested that a plausible low- z lens magnifies the true higher- z sub-mm galaxy, or that the true counterpart is identified by an alternative radio source. The CO-confirmation of the low-redshift nature of these galaxies would be an important evidence for the existence of a different starburst SED within

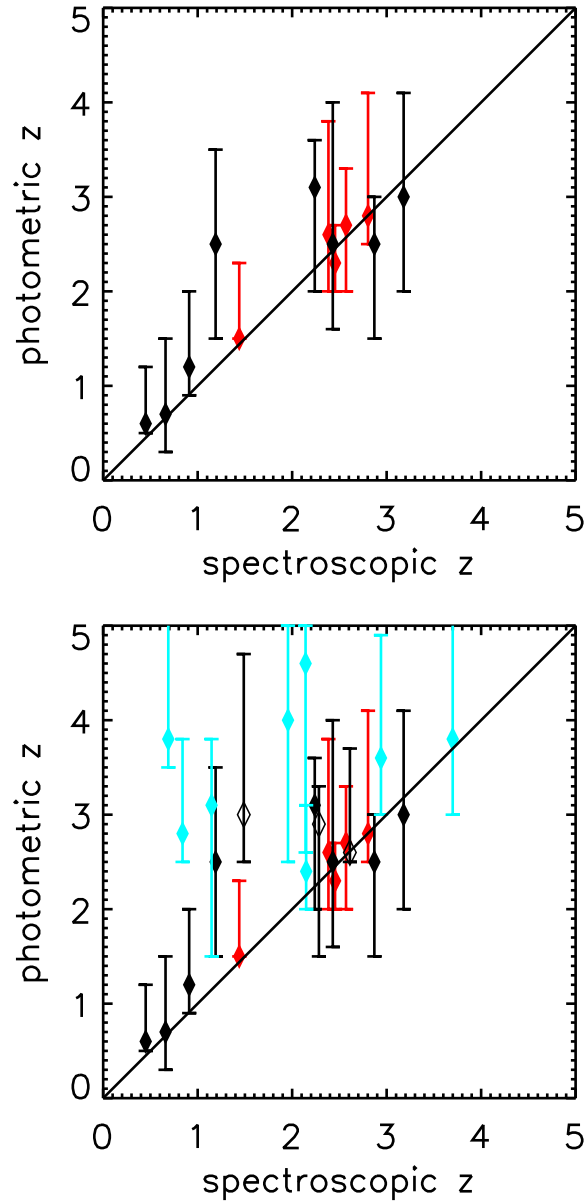


Figure 3. Comparison of spectroscopic and photometric redshifts derived from the full radio-FIR SED for a sample of 24 galaxies with accompanying multiwavelength photometry. **(Top)** Robust sample of undisputed radio/optical/IR counterpart association of the sub-mm galaxies, and spectroscopic redshifts derived from 2 or more lines: in dark grey, CO confirmed optical/IR spectroscopic redshifts; and in black, redshifts based on optical/IR spectra with two or more characteristic absorption or emission lines. **(Bottom)** The same for all 24 galaxies, where empty symbols represent optical/IR redshifts that have failed confirmation in CO, and light grey symbols correspond to galaxies with redshifts that have been disputed in the literature or that are based on one characteristic line only, and thus are not considered robust enough to be included in the sample above.

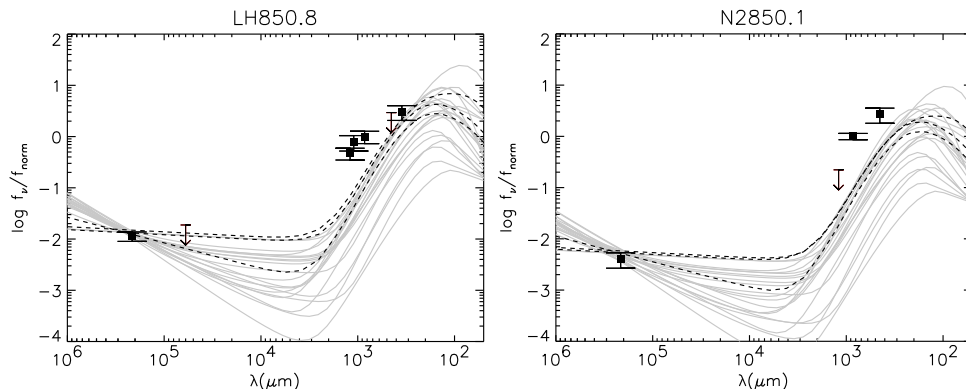


Figure 4. The observed SEDs of LH850.8 and N2850.1, normalised to the flux density at $850\mu\text{m}$ is shown as squares (detections) and arrows (3σ upper limits). The template SEDs (lines) are redshifted to their respective spectroscopic redshifts $z_{\text{spec}} = 0.689$ and $z_{\text{spec}} = 0.840$ (Chapman et al. 2005) and scaled in flux to fit the points and arrows through survival analysis. There are no template SEDs *at these redshifts*, compatible within the 3σ error bars of these objects. In light grey we represent the 20 templates of Aretxaga et al. (2003) and in dashed lines the 3 templates of Hunt & Maiolino (2005).

the sub-mm galaxy population that is not seen in the local analogs, and which should, therefore, be incorporated into the photometric redshift estimations. For the time being we consider them in the tentative category of spectroscopic redshifts.

4. Prospects

The combination of more sensitive rest-frame radio to FIR data with more complete wavelength coverage, that define the SEDs of individual galaxies identified in the next generation of FIR–radio surveys, will derive photometric-redshifts with even greater accuracy than those presented here. Furthermore, given the depth and area of these future surveys it will be extremely difficult, and often impossible, to provide useful follow-up data at optical and IR wavelengths. Thus we expect the use of photometric-redshifts to quickly increase in importance as they influence the interpretation of these new cosmological surveys.

The additional power of photometric redshifts however is their ability to efficiently select from these new FIR-radio catalogues, sub-samples of sources in well-defined redshift intervals that can be targeted by the next generation of broad-band (sub)millimetre spectroscopic receivers presented at this meeting. The future photometric redshifts from radio–FIR data will be essential in maximising the use of telescope time on facilities such as ALMA by limiting the selection of receiver tunings required to successfully search for and detect redshifted CO-lines. Since two CO-lines, identified with specific transitions, are required to unambiguously determine a spectroscopic redshift, then the combined use of a single CO-line and the photometric-redshift distribution can place important constraints on the possible frequencies that must search for

a confirming second-line (see Yun in these proceedings). The ideal solution is to combine a telescope with sufficient collecting area, to provide the sensitivity, and a millimetre spectrometer with sufficient bandwidth to always detect two CO-lines, or alternatively a CO-line and CI, regardless of the redshift of the source. The Large Millimetre Telescope (LMT) and its Redshift Receiver (Erickson – these proceedings) almost satisfy these requirements with the exception of the redshift interval ($0.5 < z < 1$ and $z \approx 2.1$ (Hughes et al. - these proceedings)).

To conclude, the different technological approaches described in this meeting to provide sensitive broad-band receivers at millimetre-wavelengths, with stable and flat spectral-baselines, will have an enormous impact on the follow-up of the most heavily-obscured continuum sources for which optical and IR techniques fail. The secure individual spectroscopic redshifts, and redshift distribution for the populations of heavily-obscured starburst galaxies, that will be derived from molecular-line emission at (sub)millimetre wavelengths, will provide critical data to understand the biases inherent in the identification of the counterparts that ultimately lead to the optical-IR spectroscopic redshifts. These CO-line data will determine the general physical properties of the gas in the molecular ISM of galaxies in the high-redshift Universe and provide estimates of their dynamical masses.

Acknowledgments. IA and DHH gratefully acknowledge support from CONACYT grants 39548-F and 39953-F to conduct their research, and from NRAO and the conference organizers to participate in this vibrant workshop.

References

- Aretxaga I. et al., 2003, MNRAS, 342, 759
 Aretxaga I., Hughes D.H., & Dunlop, J.S., 2005, MNRAS, 358, 1240
 Blain A.W., Barnard V.E., & Chapman S.C., 2003, MNRAS, 338, 733
 Carilli C.L. & Yun M.S., 1999, Ap.J., 513, L13
 Carilli C.L. & Yun M.S., 2000, Ap.J., 530, 618
 Chapman S.C., Smail I., Ivison R.J. & Blain A.W., 2002, MNRAS, 335, L17.
 Chapman S.C., Blain A.W., Smail I. & Ivison R., 2005, ApJ, 622, 772.
 Dunne L., Clements D.L. & Eales S.A., 2000, MNRAS, 319, 813
 Greve T.R. et al. 2004, MNRAS, 354, 779.
 Helou G., Soifer B.T. & Rowan-Robinson M., 1985, ApJL, 289, 7
 Hughes D.H. et al., 1998, Nat, 394, 241
 Hughes D.H. et al., 2002, MNRAS, 335, 871
 Hunt L.K. & Maiolino R. 2005, 626, L15.
 Ivison R.J. et al. 2002, MNRAS, 337, 1.
 Ivison R.J. et al. 2005, MNRAS, 364, 1025.
 Laurent G.T. et al. 2005, ApJ, 623, 742.
 Laurent G.T. et al. 2006, ApJ, 643, 1.
 Rengarajan T.N. & Takeuchi T.T., 2001, PASJ, 53, 433
 Wiklind T., 2003, ApJ, 588, 736
 Yun M.S. & Carilli C.L., 2002, ApJ, 568, 88.